ANNALS OF GEOPHYSICS, 68, 2, SY218, 2025; doi:10.4401/ag-9218
OPEN ACCESS

# Deformation and geometric change of Garisenda Tower (2010-2023): temporal variations and possible driving factors

Arianna Pesci[*,1], Giordano Teza[2], Fabiana Loddo[1], Alessandra Rossetti[1], Ilaria Gambuzzi[3], Augusto Gambuzzi[3]

(1) Istituto Nazionale di Geofisica e Vulcanologia, Sezione di Bologna, Bologna, Italy
(2) Alma Mater Studiorum – Università di Bologna, Dipartimento di Fisica e Astronomia, Bologna, Italy
(3) Studio Tecnico Dott. Ing. Augusto Gambuzzi, Modena, Italy

Article history: received December 09, 2024; accepted April 04, 2025

## Abstract

The Garisenda Tower in Bologna, standing 48 meters high with a significant inclination (~4°), is under continuous observation due to alerts from its monitoring system. The tower's structural health has been the focus of numerous studies aimed at its conservation. This article enhances the understanding of the tower's deformation state through laser scanning measurements, employing a novel approach. Unlike previous analyses that focused on individual façades, this study evaluates deformation patterns and their evolution from 2010 to 2023, considering the entire structure. The proposed method selects the statistically most reliable height bands for point cloud alignment, ensuring optimal co-registration into a common reference frame. Difference maps between multi-temporal point clouds reveal overall displacements and deformations, suggesting torsion and bending effects along the entire structure. The south side of the tower appears to be the most affected, and the overall condition in 2023 seems worse than in 2012, possibly due to the Emilia-Romagna earthquake. This new information could be valuable for planning and designing restoration interventions.

Keywords: Historical Masonry Building; Leaning Tower; Deformation; Geometric changes; Garisenda Tower

## 1. Introduction

The Asinelli and Garisenda towers in Bologna, collectively known as the Two Towers, are among the most famous ancient monuments in the world. The 97-meter-high Asinelli Tower, leaning at approximately 1°, is the tallest surviving masonry tower, while the 48-meter-high Garisenda Tower is known for its more significant inclination (~4°), so striking that it was mentioned by Dante Alighieri in the Divina Commedia (Inferno, Canto XXXI).

The lean of the towers is due to the properties of the underlying subsoil. Bologna lies on a border area between the Apennines and the Po Valley having a complex subsoil, with aquifers at various levels (Bertolini et al., 2023). Therefore, this environment is particularly sensitive to subsidence, sometimes differential on ~10 m scale and

often caused or at least amplified by anthropic interventions (Giacomelli et al., 2023; Stramondo et al., 2007; Zuccarini et al., 2024). The historic center of Bologna is especially vulnerable due to both its geology and its wealth of historical buildings, which are subjected to stresses from geophysical and atmospheric events. On the one hand, earthquakes are unpredictable phenomena both in time and intensity. On the other hand, also due to ongoing climate change, extreme weather events are expected to occur more frequently in the future.

The main results of recent observations, studies and monitoring activities carried out on the Two Towers, in some cases also including experimental modal analysis and geotechnical characterization of the soil, are reported e.g. by Baraccani et al. (2017, 2020), Marchi et al. (2022), Bertolini et al. (2023) and, focusing on remote sensing data and their integration with other information, Pesci et al. (2024). The two towers have also been the subject of static and dynamic numerical modeling but, probably due to the considerable height, most studies have concentrated on the Asinelli tower (see for example Riva et al. (1998), Baraccani et al. (2020)).

Recently, Casolino (2024) developed a static and dynamic finite element model to study the behavior of the Garisenda Tower, accounting for the limit strength values beyond which the structure would fail. The results indicated that the static and dynamic stresses on the tower are very close to these limit strengths, suggesting that in the event of a strong earthquake, the tower could suffer significant damage.

In 2023, a strain gauge installed as part of the continuous monitoring network on the Garisenda Tower provided alarming data, raising concerns about the tower's structural health (Aiello et al., 2023). This led to new investigations, immediate safety measures, and planning for potential consolidation interventions.

The above mentioned article Pesci et al. (2024) showed some remote sensing surveys carried out between 2010 and 2023, highlighting the deformations of the tower façades that occurred in this time span. It is pointed out that the term deformation means here the difference between the real geometric model (point cloud) of a building wall and the surface (plane in the case of the Garisenda tower) that should represent its theoretical shape. Furthermore, the analysis focused on the changes occurred over time, namely on the evolution of deformation patterns recognized from multi-temporal data, in particular in the case of phenomena such as earthquakes. The deformation distributions on each façade were studied in detail, but each façade was considered separately, even though the final results were discussed collectively. This study is now extended and enhanced by using the same multi-temporal data, but with a new method that provides maps of changes across the entire tower structure. The method developed here not only presents the results but also offers a criterion to overcome the limitations of relative measurements by framing the problem within a single reference system.

## 2. Section Surveys and data analysis method

The surveys were carried out by means of terrestrial laser scanning (TLS) technology. The used instrument was a long range ILRIS 3D whose specifications and performance evaluations are reported in various articles, see e.g. Pesci et al. (2013). It is important to underline that this instrument, although objectively dated, if correctly calibrated provides very accurate and stable measurement data and its performances for architectural applications are adequate to the needed precision and resolution.

The first complete survey of the external surface of the Two Towers took place in 2010 and provided the whole structure shapes as well as very interesting data about the deformation pattern of the towers' façades by means of morphological maps (Pesci et al., 2011). For each façade of each tower a morphological map was obtained as the map of differences between the corresponding point cloud and the least square plane computed from it. From here on only the results of surveys of the Garisenda tower are mentioned. The second survey was carried out in 2012, a few days after the first strong shock of the Emilia Romagna seismic sequence (https://terremoti.ingv.it/iside). Finally, the last survey was carried out in 2023, providing an almost complete geometric model of the Garisenda tower about 13 years after the first survey. Unfortunately, no measurements were carried out in the weeks immediately following the entire seismic sequence. This lack will makes it difficult to understand whether the deformations observed are entirely due to the earthquake or whether there is some other ongoing phenomenon, as suggested by the activated alarm from continuous system.

Each tower model consists of the point clouds needed to cover the entire area, acquired strategically to minimize alignment errors. To ensure excellent alignment in generating the complete point cloud, every single scan taken from one of the four station points around the tower completely covered two adjacent façades (Fig. 1). This ensures a very high overlap between the partial point clouds (Pesci et al., 2013).

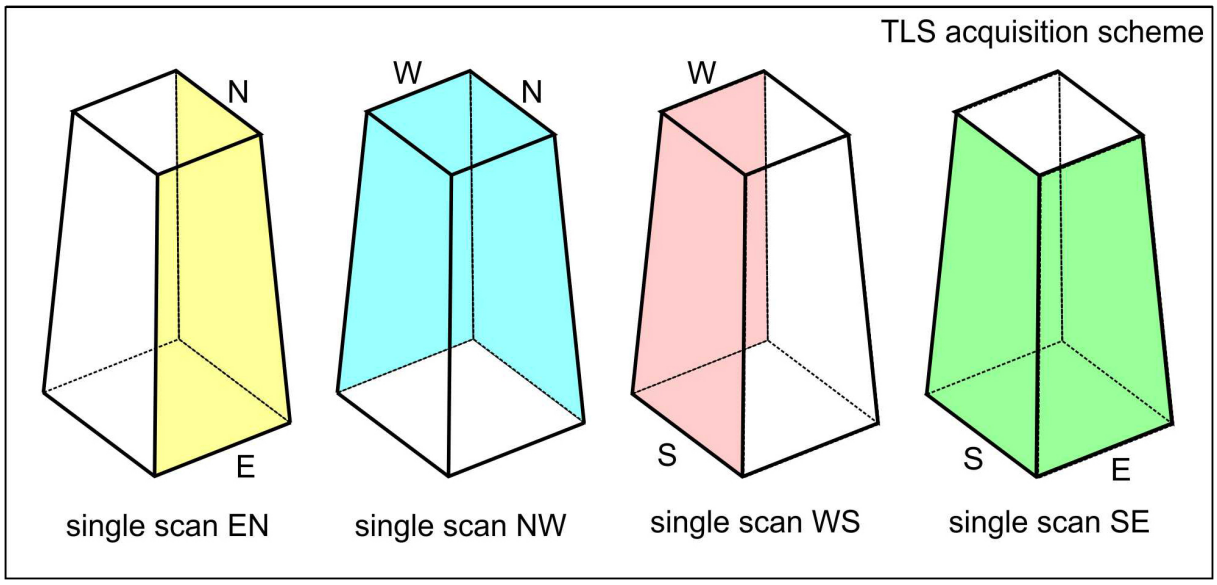


**Figure 1.** Acquisition scheme for a TLS survey. Each single scan covered two façades at the same time. Four observation points around the tower were considered.

In order to evaluate the changes over time, the multi-temporal point clouds must be aligned with each other. For this purpose, taking the 2010 point cloud as the reference model, all other point clouds were aligned to it. Since the lower part of the tower (~10 m high) was obscured by scaffolding in 2023, the corresponding points were excluded from the alignment process across all multi-temporal point clouds to ensure consistent boundary conditions in each analysis.

As stated, the first published study was aimed at the evolution with time of the morphological map of each individual façade of the tower in order to recognize possible changes. To carry out this, for each survey four independent point clouds related to the North (N), East (E), South (S) and West (W) façade were obtained by cropping the corresponding whole point cloud. Subsequently, for each façade these multi-temporal partial point clouds were aligned and compared with respect to the reference plane obtained by means of least square fitting of the points belonging to the 2010 one. At first glance this reference plane would seem like an arbitrary choice. However, it is the ideal surface most similar to the prospect in question and, therefore, more suitable to the recognition of deviations from the ideal shape that could be due to static or dynamic loads that affected the structure over time, or anthropic. For each façade, the 2010, 2012 and 2023 multi-temporal morphological maps were computed, also allowing the recognition of the areas most sensitive to earthquake. Furthermore, it was possible to compare the current state to the 2010 one, therefore considering a 13 years cumulative condition (Pesci et al., 2024). Finally, it should be noted that this analysis, based on remote sensing data, concerns only the outer layer of the monument.

The main results presented in Pesci et al. (2024) are briefly summarized in Fig. 2:

1) Positive deformations (i.e., out-of-plane) in the upper part of the N façade (above 32 m) emerged in 2012 as a consequence of the earthquake. These deformations partially reverted over time. However, due to the lack of surveys between 2012 and 2023, it is not possible to determine when this partial recovery occurred (in the case of the Asinelli Tower, earthquake-induced deformations disappeared a few months after the end of the seismic sequence (Pesci et al., 2013)).
2) A twisting of the upper part (above 40 m) and a reduction in point-to-plane distance above 25 m were observed on the N façade.
3) A positive (out-of-plane) deformation appeared above 45 m on the E façade.
4) A negative (in-plane) deformation at the summit of the W façade was observed, along with evidence of earthquake sensitivity in the section above 30 m.

The analysis presented so far enables the recognition and evaluation of possible deformations on each individual façade relative to an ideal surface (the corresponding least-squares plane in the case of the Garisenda). In the case of multi-temporal data, it also allows for the detection of any changes over time. However, this approach

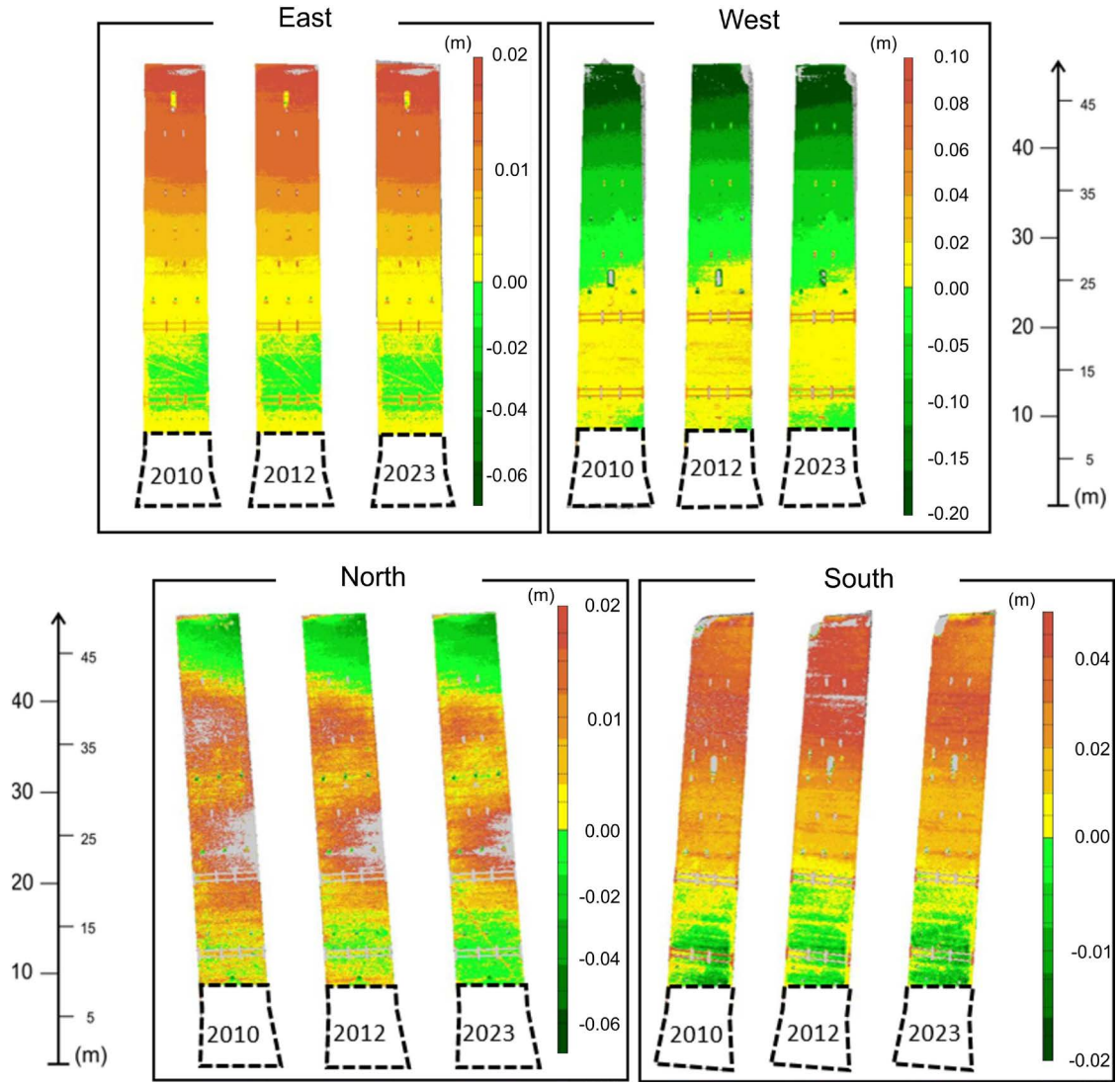


**Figure 2.** Multi-temporal morphological analysis of Garisenda tower façades, modified from Pesci et al. (2024).

does not account for rigid body movements or deformations involving multiple parts of the tower simultaneously. This limitation prevents a comprehensive description of the actual deformations. Therefore, a specific analysis method was required to minimize systematic effects and achieve a more complete observation of the tower's overall deformation framework.

The surveys were carried out without data georeferencing, an operation that was deemed not essential at the time of the first survey. The measurements are relative and not obtained in the same reference system needing alignment before direct comparison. Following the registration of all the multi-temporal models into a same reference frame (the one of 2010 first model) direct comparison is possible. It is necessary to warrant that the point cloud portions used for alignment are always the corresponding ones in every comparison procedure. Given that the lowest part (below 10 m) of the 2023 model is missing because of scaffolds, it was also ignored in the processing of 2010 and 2012 models. Furthermore, the point clouds were "regularized" in order to consider models characterized by the same sampling step and therefore having very similar contents of points. After the control and regularization operations, the three models can be finally compared looking for the best strategy for a subsequent interpretation. The method used for data analysis cannot ignore the fact that the same models must be used both for alignment and for the study of differences as the alignment is carried out. In order not to fall into a logical error due to the use of the same data to formulate a given hypothesis and to test its validity, we proceed by elevation bands, from the bottom to the top of the tower or from the top to the bottom. To keep this article lean, and to clarify how the method is structured and can be used, it is directly described through the specific application in the next section dedicated to the results.

All data processing, both for the generation and analysis of the multi-temporal morphological maps described in Pesci et al. (2024), and for the processing and analysis of the complete multi-temporal point clouds presented in this article, was carried out using the PolyWorks software package (https://www.innovmetric.com/products/polyworks-inspector).

Finally, it is emphasized that this kind of analysis, which uses non-georeferenced data, cannot recognize possible rigid body movements. The procedures used here were designed to overcome the lack of georeferencing (it should be noted that the initial objective of the 2010 and 2012 surveys was not to obtain georeferenced models, but to evaluate the behavior of the tower façades). In a series of surveys of a highly valuable historical building is planned, it may be useful to use a network of ground control points or also, where possible, direct georeferencing (Turnet et al., 2014). However, the method described here applies in all those cases in which there are previous non-georeferenced data or in which georeferencing is problematic or there are obstacles to it.

## 3. Results

The 2010 model was locked into its reference system and used as the reference model. Because of the above mentioned reason (presence of scaffolds in 2023), the points below 10 m height were inhibited for alignment procedures. Therefore, no more than ~83% of the tower model can be used. The case where all the tower above 10 m is called Case 0 here. This case corresponds to the most complete comparison in which the alignment algorithm works to minimize the distance between the two models along the local normal directions. Case 0 suffers from two problems, however. On the one hand, if the deformed parts are very large compared to the total, the result could represent an unrealistic condition. On the other hand, the subsequent comparison would be based on the same points used for the alignment, giving rise to a problem of lack of scientific meaning of the result. For this reason, some additional cases are considered by varying the parts used to align the multi-temporal point clouds: Case 1, where all the points in the height interval between 10 m and 25 m are used; Case 2, where all the points in the height interval between 10 m and 25 m are used; Case 3, where all the points in the height interval between 10 m and 30 m are used; Case 4, where all the points in the height interval between 10 m and 40 m are used. The cited cases represent bands of overlap that vary between 31% (the minimum to have a good alignment) and 83% of the entire tower. The main results of the analyses, in terms of means and standard deviations (SDs), are summarized in Table 1, where data about other height ranges are also shown. Table 2 summarizes the results of similar analyses carried out starting, for the alignment, from the tower top. As expected on the basis of results shown in Fig. 2 about the single façades, the values in Table 2 are quite different from the Table 1 ones because the deformations tend to increase as the reached elevation increases. The results of the statistical analysis summarized in Tables 1 and 2 are also shown in Fig. 3.

The analysis of 2023 to 2010 differences shows that both means and SDs increase as the overlap percentages for the alignment increase and that these values are greater than the ones from 2012 to 2010 comparison. This fact suggests the presence of a larger fraction of altered and deformed area, which means that a large amount of points belonging to the point cloud representing the tower body influences the alignment and subsequent analysis.

It is very interesting to evaluate the results as maps of the differences between models. Figure 4 shows all the results for all the considered cases as North-East (NE) and South-West (SW) views of the 2010 tower point cloud colored with a scale representing differences in the range ±2cm.

Case 0 and Case 1 represent the two limit conditions for model alignment, where the fractions of used points are 83% and 31% respectively. In the hypothesis, which is supported by what is show in Fig. 3, that the lower bands are less affected by deformation, these limit cases represent the total adjustment where each part of the tower contributes (Case 0) and the partial adjustment with a targeted and safer selection (Case 1). The fact that in the 2023-2010 comparison the two cases reveal significant differences should be noted. In particular, the N side of Case 1 shows positive values even higher than 2.5 cm and, clearly, less positive values on the S side. This does not happen, however, in the 2012-2010 comparisons where the discrepancies between the two extreme cases are smaller. Considering the deformations on the walls shown in Fig. 5, which show that the N and S walls seem do not have coupled behavior, and also considering that an overlapping area of at least 30% is enough to guarantee a correct alignment, the obtained result is a possible symptom of a deformation increase for the whole tower body. Table 1 and Fig. 4 also show the results obtained in other cases, with different overlap fractions. A statistical analysis of the results show that the better compromise between a large overlap and avoiding the effects of deformation is achieved

| Bottom → Top | | | | 2012-2010 | | 2023-2010 | |
|---|---|---|---|---|---|---|---|
| Case | Interval (m) | Overlap (m) | Tower perc. (%) | Mean (mm) | SD (mm) | Mean (mm) | SD (mm) |
| | (10:15) | 5 | 10 | −0.6 | 6.0 | −0.6 | 6.5 |
| | (10:20) | 10 | 21 | −1.5 | 6.5 | −1.0 | 7.5 |
| Case 1 | (10:25) | 15 | 31 | −1.5 | 6.5 | −0.6 | 7.0 |
| Case 2 | (10:30) | 20 | 42 | −0.6 | 6.5 | 0.6 | 7.5 |
| Case 3 | (10:35) | 25 | 52 | −0.2 | 6.5 | 1.0 | 7.5 |
| Case 4 | (10:40) | 30 | 63 | 0.2 | 7.5 | 2.0 | 7.5 |
| | (10:45) | 35 | 73 | 1.0 | 8.0 | 3.5 | 7.5 |
| Case 0 | (10:48) | 38 | 83 | 1.0 | 9.0 | 4.5 | 8.5 |

**Table 1.** Comparison of multi-temporal 3D models using variable alignment areas, progressively enlarging the overlapping region from the bottom upward. Overlapping bands are defined by vertical interval levels. Case 0 includes the entire tower above 10 m (83% of the tower body used), while Case 1 focuses on a 15 m band in the lower portion of the tower (31% of the total), common to both the 2023 and 2010 point clouds. Although results (mean and standard deviation) are similar between cases, they are not identical due to the impact of deformation. As deformation increases in the upper regions, both mean and standard deviation (SD) tend to increase.

| Top → Bottom | | | | 2012-2010 | | 2023-2010 | |
|---|---|---|---|---|---|---|---|
| Case | Interval (m) | Overlap (m) | Tower perc. (%) | Mean (mm) | SD (mm) | Mean (mm) | SD (mm) |
| | (48:43) | 5 | 10 | 5 | 15 | 10 | 12 |
| | (48:38) | 10 | 21 | 4 | 13 | 9 | 10 |
| | (48:33) | 15 | 31 | 3 | 11 | 8.0 | 9.5 |
| | (48:28) | 20 | 42 | 3 | 11 | 7.0 | 9.0 |
| | (48:23) | 25 | 52 | 2 | 10 | 6.5 | 9.0 |
| | (48:18) | 30 | 63 | 2 | 10 | 6.5 | 8.5 |
| | (48:13) | 35 | 73 | 2 | 10 | 5.5 | 8.5 |
| Case 0 | (48:10) | 38 | 83 | 1 | 9 | 4.5 | 8.5 |

**Table 2.** Comparison of multi-temporal 3D models using variable alignment areas, progressively enlarging the overlapping region from the top downward. Overlapping bands are defined by vertical interval levels. Case 0 includes the entire tower above 10 m (83% of the tower body used).

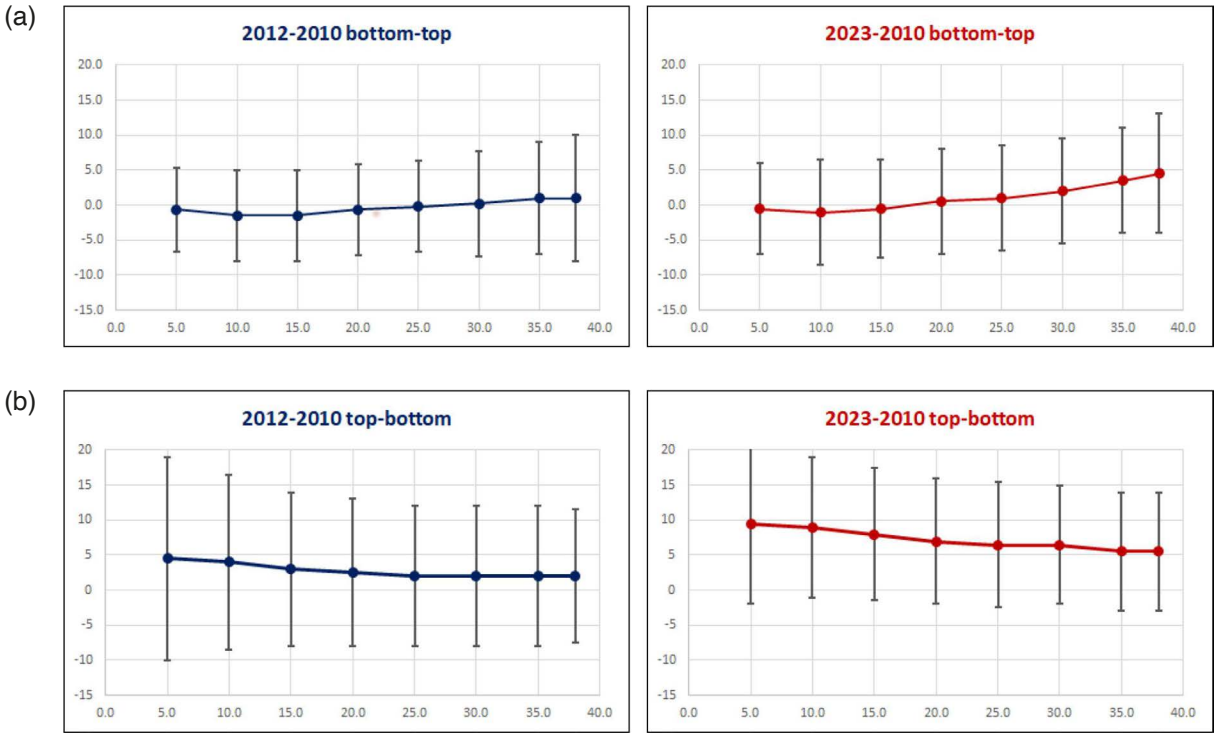


**Figure 3.** Results of statistical analysis of the differences between aligned multi-temporal point clouds in terms of means (points) and SDs (error bars) obtained comparing 2023 and 2012 models to the 2010 reference one. The graphs show the data from Tables 1 and 2, and are obtained by selecting increasingly larger point cloud portions for alignment with a step of 5 m both proceeding from bottom to top (a) and from top to bottom (b).

in Case 2, where the elevation range is between 10 and 30 m and the overlap fraction is 42%. The model colored with the differences with respect to the reference 2010 one are shown in Fig. 5.

The distribution of the differences shown in Figs. 4 and 5 allow the recognition of torsion and bending effects due to 2012 earthquake. The condition observed in 2023 is characterized by more extensive and differential changes, in which diagonal patterns can also be recognized. It should also be remembered that possible rigid body movements cannot be highlighted with the used method.

Finally, additional information of a hybrid but interesting nature is presented. Starting from Case 1, i.e., from the models of the tower aligned in a realistic manner, each façade is compared to the plane fitted using the 2010 point cloud. The multi-temporal series of the newly co-registered morphological maps is shown in Fig. 6, where the color scale is chosen to maximize the contrast between positive and negative values. Compared to the results presented in Fig. 2, where all façades are considered independently, here the morphological maps are influenced by the general layout of the tower. The term “hybrid” is used because the values and value patterns shown do not represent individual wall configurations but rather each wall in relation to a hypothetical regular model (a plane) defined by the 2010 data. Therefore, for each façade, the results depend on both its cumulative deformation and its displacement relative to the initial position, as a result of changes in the entire tower body.

To more directly evaluate the deformations suffered by the tower with consequent morphological and structural change, Fig. 7 shows some cross-sections related to Case 2 (height interval for alignment: 10-30 m, 42% of points). Two horizontal cross-sections at 10 m and 38 m height respectively allow a representation of the changes which occurred with time. The three used colors correspond to the different epochs: black for 2010, red for 2012 and green for 2023.

Essentially, once the most reliable alignment is achieved, there are various ways to interpret the results, either by directly examining the differences between co-registered models or by analyzing the changes over time in morphological patterns. Previously, only the independent deformations of the façades were evaluated; these results were not highly sensitive to the reference system but were indicative of ongoing phenomena.

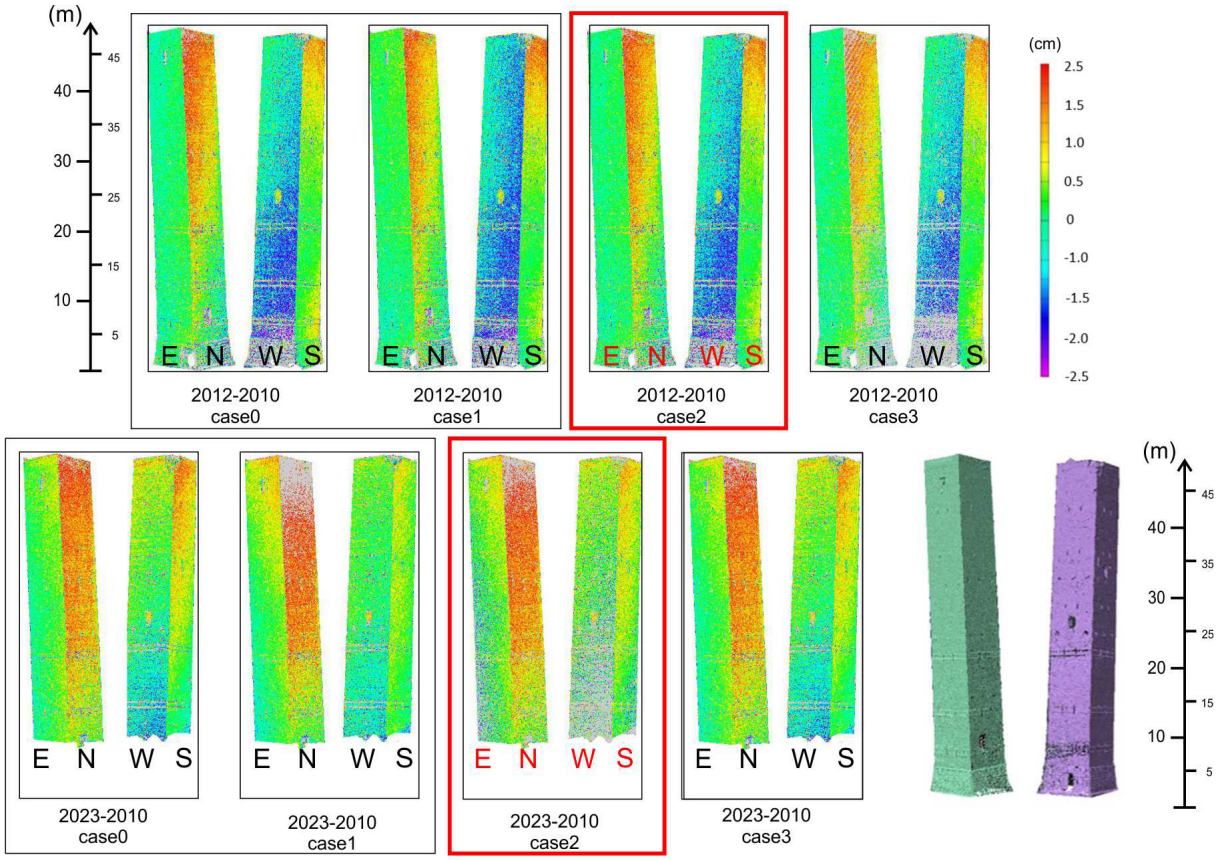


**Figure 4.** Differences between multi-temporal models and the reference 2010 one. The NE and SW façades are shown side by side. The boxes show the cases for the 2012-2010 comparison and for the 2023-2010 comparison. Please remember that Case 0 represents the alignment of everything with everything while Case 1 is treated with points in the band between 10 and 20 m high. Case 2 (red framed) represents the best one from statistical results about alignment. The views are chosen in order to better show the distribution of the differences on the tower body.

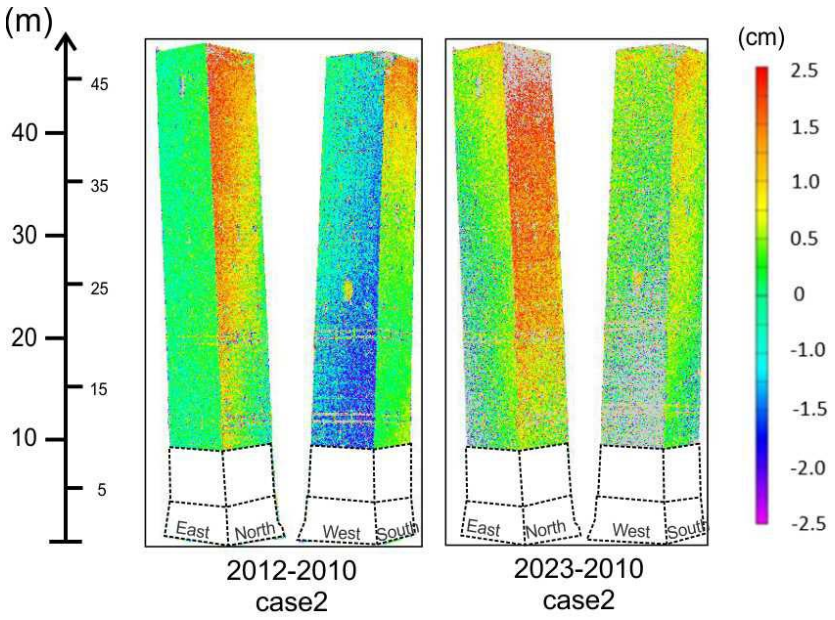


**Figure 5.** Maps of differences between multi-temporal models with respect to the reference 2010 one (Case 2, 42% overlap for the point cloud alignment). The lower part is blanked because excluded from alignment.

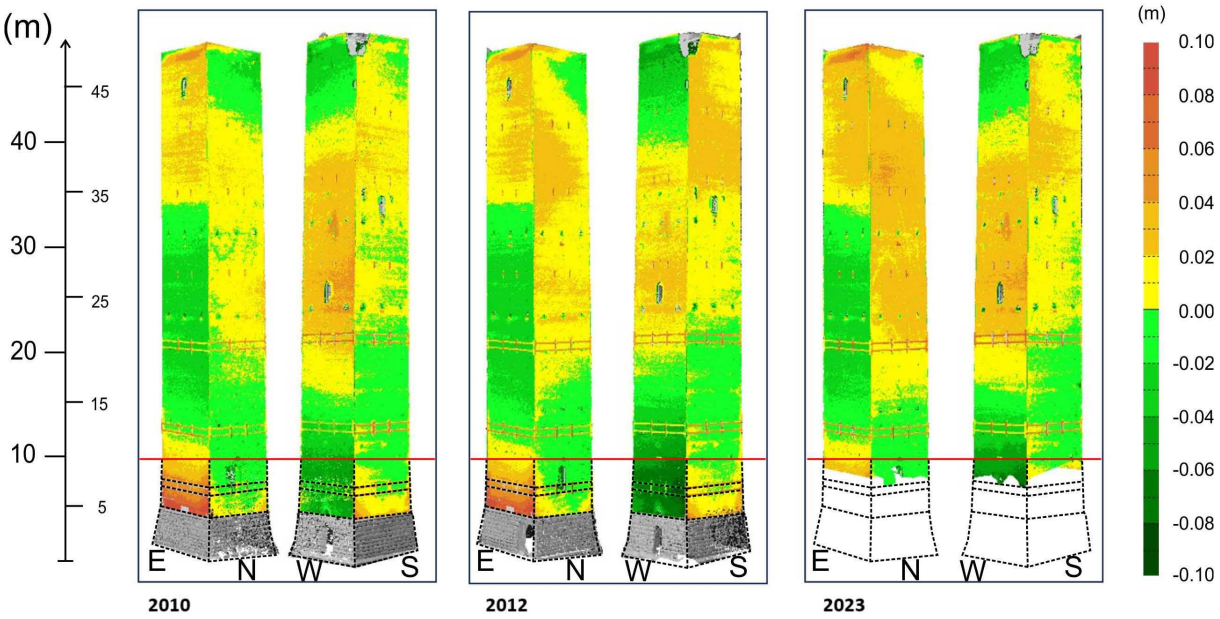


**Figure 6.** Morphological maps of tower façades obtained with respect to the 2010 ideal planes. Under the red line no points are considered for alignment process.

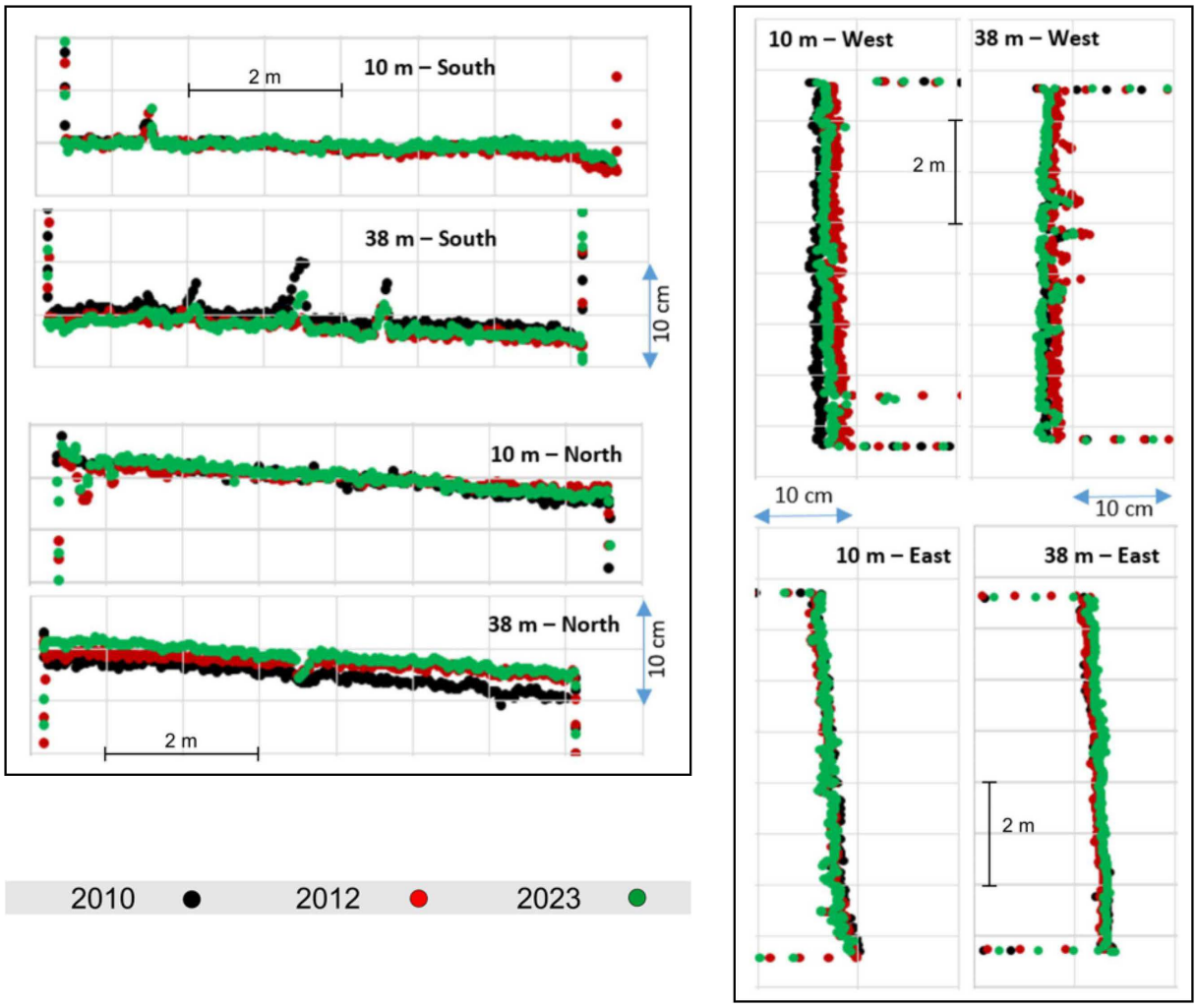


**Figure 7.** Cross sections extracted at 10 m and 38 m high levels of multi-temporal point clouds.

## 4. Discussion and conclusions

The deformation analysis of the Garisenda Tower, performed through Terrestrial Laser Scanning (TLS) over multiple years (2010, 2012, 2023), was carried out using a multi-step process as outlined in Fig. 8. The diagram provides a visual summary of the methodology, detailing the stages of TLS scans, model alignment, and comparison to detect deformations over time. This method, which relies on precise registration and integration of multi-temporal point clouds, allows for the observation of subtle changes in the tower's geometry.

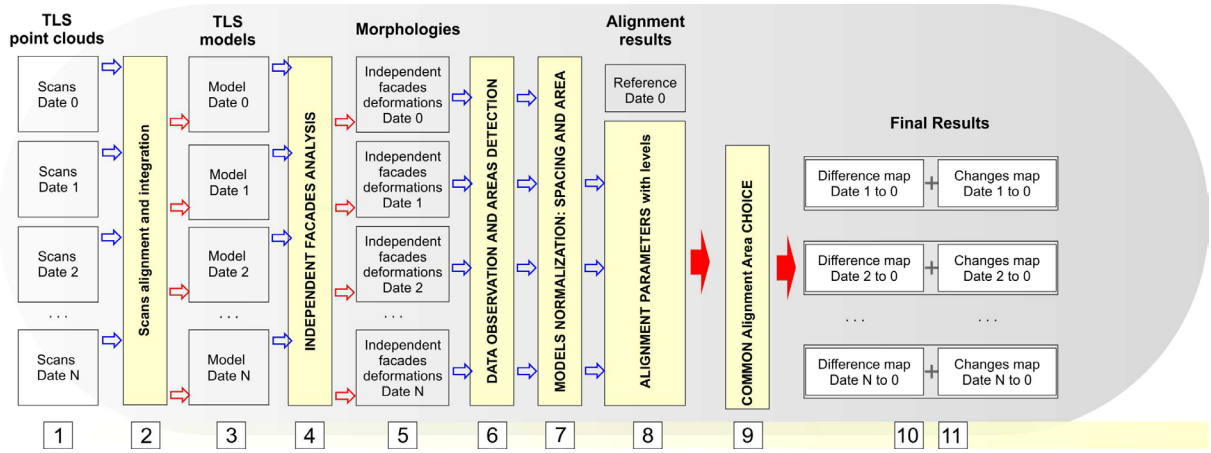


**Figure 8.** Flowchart of the deformation analysis of the Garisenda Tower using TLS scans and multi-temporal models. The diagram outlines the main steps of the process, starting with the initial TLS scans (column 1) and concluding with the generation of difference and change maps (final column). The scans are first aligned and integrated (column 2), then analyzed independently for each facade (column 4). The facades' morphologies are calculated and compared over time (column 5), followed by data observation and model normalization actions (subsequent columns). The normalized models are then sequentially compared using variable common areas (column 7) to determine the best alignment parameters (column 8) and the corresponding alignment area (column 9). Finally, the alignment results are presented as direct model differences (column 10) and changes maps showing the differences between points and the fit plane from the reference model (column 11).

The results of this extended analysis show variations within a 5 cm range, and the 2012-2010 difference maps (Fig. 5) suggest that some of the observed variations may have been induced by the first seismic shock of the 2012 Emilia-Romagna seismic sequence. In addition to the direct deformations suffered by the individual façades (Fig. 2, already shown in Pesci et al. (2024)), a global torsional and bending pattern is visible, particularly in the higher part of the tower. The 2023-2010 comparison highlights an accentuation of the differences, especially on the N side, and the maps show different patterns compared to the 2012-2010 ones. This is clearly visible in Figs. 6 and 7. In particular, the multi-temporal morphology obtained by comparing the models with the four least square fit planes of the 2010 façades shows a deformation progression (Fig. 6). Figure 7 shows the results of a direct extraction of horizontal cross-sections at 10 m and 38 m, highlighting the changes that occurred along well-defined lines.

One of the challenges in this analysis is the identification of an optimal method for the registration of all the multi-temporal models into a common reference frame. Due to the lack of georeferencing (which was not possible in this case), the nature of remote sensing data is relative rather than absolute. The choice of the area for the co-registration of multi-temporal point clouds was based on four key factors: (i) a good alignment should involve at least 30% of the points; (ii) the deformation is more pronounced as the height of the point cloud portion considered increases; (iii) missing areas in one of the point clouds must be excluded in all subsequent comparisons; (iv) subsequent comparisons must use already-aligned data, creating a logical challenge if all points are used. In the case of Garisenda, statistical analyses suggested aligning the scans between 10 m and 30 m (Case 2), which seems to be the best compromise between these opposing needs. It is important to note that the changes detected across

the entire tower should be interpreted as the most realistic variations possible, as if the instrument had been fixed at four observation points in 2010 and kept as consistent as possible in the subsequent surveys.

The 2012-2010 and 2023-2010 difference patterns, together with the independent variations for each façade, reveal effects attributable to torsion and bending phenomena. These phenomena are particularly significant on the N and S façades but are also visible on the W and E ones. Although these results provide valuable insights, a definitive interpretation is challenging due to the relative nature of the measurements and methodology. The current state of the tower could be the result of the 2012 seismic sequence, but other ongoing phenomena cannot be excluded. Notably, a strain gauge continuously monitoring the tower base has shown that a drift effect (negative deformation) started in 2022. Furthermore, for several months now, the Garisenda Tower has been surrounded by a protective barrier, made of large containers stacked along its entire perimeter. This has prevented any further measurements to observe ongoing phenomena.

A final note about the role of temperature and solar effects on the tower. There is no doubt that temperature variations and solar radiation influence the natural vibration modes of the tower (see, for example, Vitiello et al., 2020). However, these effects occur at frequencies and amplitudes too small to be detected by terrestrial laser scanning (TLS), where metric measurements dominate. In practice, temperature-induced vibrations remain within the TLS data noise due to their high frequency and small displacement, negligible compared to the centimeter-scale precision of the scans. Detecting such movements would require a terrestrial InSAR system. Moreover, the tower's massive structure, with materials of high thermal capacity and low conductivity, minimizes thermal expansion. The timing of the scans, performed in stable early morning conditions, further reduces the impact of temperature fluctuations. As a result, TLS scans primarily capture long-term deformations from sources like seismic events, rather than temperature-induced effects. Historical evidence from Cavani (1903), monitoring the top of the tower over a year, confirms that temperature-induced displacements were minimal and did not affect the tower's stability. These observations support the conclusion that temperature variations do not interfere with TLS measurements due to the nature of the technique, the acquisition times, scanning method, sampling step, ground signal footprint, and measurement redundancy.

Future developments will focus on numerical modeling, particularly optimizing static and dynamic finite element models, building upon the work of Casolino (2024), and incorporating the deformations obtained with the described approach. The method presented here can also be applied to other cases where multi-temporal models of tall buildings are available but lack georeferencing or have insufficient precision for meaningful comparisons.

**Data availability statement.** The laser scanning surveys were carried out by the authors. These data may be shared upon reasonable requests. All other data and information were taken from the sources reported in the References.

**Acknowledgements.** The activities were financed by Istituto Nazionale di Geofisica e Vulcanologia within the framework of the "Ricerca Libera Rescue Project" (www.ingv.it/ricerca/progetti-e-convenzioni/progetti). The authors wish to thank Giorgia Casolino (University of Florence) for a very helpful discussion about the results of numerical modeling of the Garisenda tower.

## References

Aiello, E., A. Bellini, G. Capponi, A. Di Tommaso et al. (2023). Relazione Tecnica del Comitato Tecnico Scientifico per il consolidamento della Torre Garisenda (come da richiesta dell'ill.mo Sindaco del 23 Ottobre 2023), Comune di Bologna, Bologna, https://static.gedidigital.it/repubblica/pdf/2023/locali/bologna/relazione_tecnica_finale_cts_151123.pdf.

Baraccani, S., M. R. Azzara, M. Palermo, G. Gasparini et al. (2020). Long-term seismometric monitoring of the two towers of Bologna (Italy): Modal frequencies identification and effects due to traffic induced vibrations, Front. Built Environ., 6, 85, doi:10.3389/fbuil.2020.00085.

Baraccani, S., M. Palermo, G. Gasparini, S. Silvestri et al. (2017). The seismic assessment of the Asinelli tower in Bologna, in Proc. of 16th World Conference on Earthquake, 16WCEE, Santiago, Chile, 2068, 1-12, https://www.wcee.nicee.org/wcee/article/16WCEE/WCEE2017-2068.pdf.

Bertolini, I., M. Marchi and G. Gottardi (2023). Learning from a Well-documented Geotechnical Cold Case: The Two Towers of Bologna, Italy, Int. J. Archit. Herit., 17, 10, 1607-1629, doi:10.1080/15583058.2022.2057828.

Casolino, G. (2024). Analisi dello stato deformativo e tensionale della torre Garisenda a Bologna, Relatori R. Nudo Correlatore: M. Tanganelli, Università degli Studi di Firenze, Scuola di Architettura, Firenze.

Cavani, F. (1903). Pendenza, stabilità e movimenti delle torri la Garisenda di Bologna e la Ghirlandina di Modena, Tipografia Gamberini e Parmeggiani, Bologna, 58, 11, ISSN: MOD0377865.

Giacomelli, S., A. Zuccarini, A. Amorosi, L. Bruno et al. (2023). 3D geological modelling of the Bologna urban area (Italy), Eng. Geol., 324, 107242, doi:10.1016/j.enggeo.2023.107242.

Marchi, M., I. Bertolini and G. Gottardi (2022). A geotechnical insight into the soil-foundation system of the Two Towers of Bologna, Italy, Geotechnical Engineering for the Preservation of Monuments and Historic Sites III, 631-642, doi:10.1201/9781003308867.

Pesci, A., G. Teza, F. Loddo, A. Rossetti et al. (2024). The role of remote sensing to enlarge knowledge on health state of a historical building hit by earthquake: The case of Garisenda leaning tower (Bologna), Ann. Geophys., 67, 5, S550, doi:10.4401/ag-9119.

Pesci, A., G. Teza, E. Bonali, G. Casula et al. (2013). A laser scanning-based method for fast estimation of seismic-induced building deformations, ISPRS J. Photogramm. Remote Sens., 79, 185-198, doi:10.1016/j.isprsjprs.2013.02.021.

Pesci, A., G. Casula and E. Boschi (2011). Laser scanning the Garisenda and Asinelli towers in Bologna (Italy): detailed deformation patterns of two ancient leaning buildings, J. Cult. Herit., 12, 2, 117-127, doi:10.1016/j.culher.2011.01.002.

Riva, P., F. Perotti, E. Guidoboni and E. Boschi (1998). Seismic analysis of the Asinelli Tower and earthquakes in Bologna, Soil Dyn. Earthq. Eng., 17, 525-550, doi:10.1016/S0267-7261(98)00009-8.

Stramondo, S., M. Saroli, C. Tolomei, M. Moro et al. (2007). Surface movements in Bologna (Po Plain – Italy) detected by multitemporal DInSAR, Remote Sens. Environ., 110, 3, 304-316, doi:10.1016/j.rse.2007.02.023.

Turner, D., A. Lucieer and L. Wallace (2014). Direct georeferencing of ultrahigh-resolution UAV imagery, IEEE T. Geosci. Remote Sens., 52, 5, 2738-2745, doi:10.1109/TGRS.2013.2265295.

Vitiello, V., R. Castelluccio and M. Del Rio Merino (2020). Experimental research to evaluate the percentage change of thermal and mechanical performances of bricks in historical buildings due to moisture, Constr. Build. Mater., 244, 118107, doi:10.1016/j.conbuildmat.2020.118107.

Zuccarini, A., S. Giacomelli, P. Severi and M. Berti (2024). Long-term spatiotemporal evolution of land subsidence in the urban area of Bologna, Italy. Bull. Eng. Geol. Environ., 83, 35, doi:10.1007/s10064-023-03517-5.

***CORRESPONDING AUTHOR: Arianna PESCI**,
Istituto Nazionale di Geofisica e Vulcanologia, Sezione di Bologna, Bologna, Italy
e-mail: arianna.pesci@ingv.it